

Rotating microflow sensors

Rafaele Attia,^a Daniel C. Pregibon^b, Patrick S. Doyle,^b Denis Bartolo^c, Jean-Louis Viovy,^a

Received (in XXX, XXX) 1st January 2007, Accepted 1st

5 January 2007

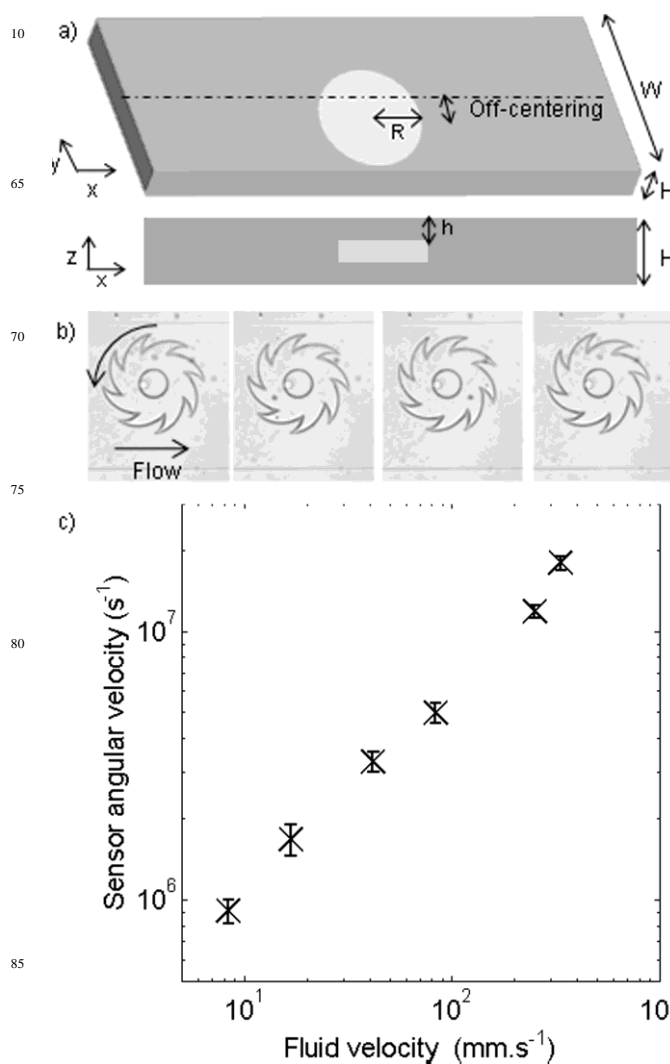
First published on the web 1st January 2007

DOI: 10.1039/b000000x

We present a microflow sensor based on the rotation of a wheel around an axle. The sensor is implemented *in situ* in a PDMS microchannel with Stop Flow Lithography (SFL)[1] of a photocurable monomer. The response of the resulting “plastic MEMS” depends neither on the fluid’s viscosity, nor on other physico-chemical properties such as the thermal conductivity. Consequently, this type of flow sensor alleviates the need for recalibration whenever different fluids are to be used in the same device. The measurable flow range for a given wheel design is three orders of magnitude. We also introduce a simple model and a numerical simulation which are in excellent agreement with experimental results. The model can be used to design the geometry of the system in order to tune the measurable flow rate to the desired range of values.

Introduction

30 Measuring flow rates is a serious challenge in microfluidics, in which very small fluid volumes and flow rates in the range of nl/min are typical. The flow sensing methods currently used in microfluidics mainly belong to four main categories. The most widely used involve indirect measurements. (i) In a first option, the pressure drop across a calibrated strait can be used. The main limitation of this approach lies in the pressure measurement itself: most pressure sensors involve the displacement of a meniscus located between the microchannel and the sensor itself. Because of the small dimensions, the Laplace pressure across this meniscus may be quite significant, and alter the measurement. In addition, due to inevitable contact angle hysteresis, the meniscus motion may induce significant hysteresis in the pressure measurement. (ii) The second and more common option is based on a measure of the thermal response of the flowing fluid locally heated with a hot wire. As a strong advantage, this method is contactless, so it can be performed in glass capillaries (2). It has, however, still several disadvantages. First, the measurable flow range is rather limited, at most two orders of magnitude. Second, the response time is slow; and third the measure depends on the thermal capacity of the fluid. Thus, this method requires a preliminary calibration or an independent measure for each different fluid used. (iii) Particle Imaging Velocimetry is the third common option to perform flow measurement (3). In principle, this direct approach provides an absolute and fluid-independent measure of the flow rate, since the particles are convected at the fluid velocity. However, the need to seed the fluid with tracers is a strong limitation, in particular for routine applications. Furthermore, pressure driven channel flow of fluids will have a Poiseuille velocity profile, so a full velocity profile across a microchannel section must be accurately recorded and integrated to determine the overall flow rate. Additionally,



90 **Fig. 1:** a) sketch of the sensor geometry b) Image sequence of a micro-wheel based flow sensor (total time: 4 s, outer diameter: 360 μm). The rotation is induced by a silicone oil flow (viscosity 20 cp, flow rate 50 $\mu\text{l}/\text{min}$). c) Angular velocity of the spinning wheel plotted versus the mean fluid velocity ($\mu=100\text{cP}$)

PIV equipments require a high quality imaging, they are expensive and the need for high resolution imaging itself puts strong constraints on the design of the microchip. (iv) As an alternative to these approaches, we recently proposed a new family of microspring flow sensors. They are based on the elongation of a deformable structure polymerized inside a microchannel thanks to a microscope-based Soft Flow Lithography technique (4). This type of sensor does not require tracers, it can measure flow velocity over four orders of magnitude, and it can be fabricated at very low cost. As a limitation, however, this sensor requires the knowledge of the fluid viscosity. Although this physical property is rather easy to measure, it varies significantly with temperature, which can

be detrimental when the temperature of the device must be changed during chip operation.

Here, we introduce a new type of flow sensor that overcomes most of the aforementioned limitations. This new device relies on a very simple MEMS-like structure. The flow measurement is achieved by monitoring the rotation rate of a polymerized plastic wheel, which freely moves around a fixed axle. It retains the simplicity of fabrication and operation of “microspring” flow sensors, but does not require the *a priori* knowledge of any fluid property; thus providing a truly universal flow measurement. In the following, we explain the rationale underlying the design of the flow sensor, we investigate its performance with a variety of fluids, and finally, we compare our results with a theoretical model that provides simple guidelines to design flow sensors suited to a predefined range of flow rates. The experimental details are given at the end of the paper.

Principle

The sensing element of our system is a circular wheel, able to freely rotate around a fixed axle (Fig 1a) and located in a straight and wide microchannel. In order to induce a torque, the flow profile must be asymmetric. This is achieved by setting the wheel off-center in the channel. Because of the very low Reynolds numbers encountered in microchannels, viscous coupling is strong, and at a given stationary flow rate, the flow profiles are independent of viscosity, thus leading to viscosity-independent dynamics (see “modeling” section for a more detailed explanation). Practically, the wheel is photopolymerized *in situ* in the microchannel. In brief, a mask is placed in the focal plane of a classic inverted microscope and a prepolymer solution is exposed to the projected UV light (see “Experimental” for details). Due to oxygen diffusion through the walls of the microchannel, a non-polymerized layer surrounds the wheel, so that it does not stick to the channel walls or to the axle (which is also made of PDMS). These minimal plastic MEMS features cannot translate (because of the axle) but can freely rotate in the channel (see Supplementary Material movie). Next, the non-polymerized solution is replaced by a given fluid and the rotational velocity is optically measured from the speed of a small spot feature embedded in the sensor’s design, as shown in Fig.1. Different wheel shapes and sizes were made and successfully tested.

Flow Sensor characterization

A first measure of sensor angular velocity is given in Fig 1c. Within experimental error, the angular velocity is linear as a function of fluid velocity (imposed by a high accuracy syringe pump), which validates the principle of operation of the sensor. To further validate our design strategy, we investigated the dependence of the measured velocity on the fluid viscosity. We first flowed several silicone oils with calibrated viscosities. By doing so, we varied only the viscosity of the tested fluid without changing any other physico-chemical property. The sensor angular velocities as a function of flow rate collapse on the same linear master curve for all the tested fluids over three flow decades (Fig. 2). The minimum measurable flow rate is limited

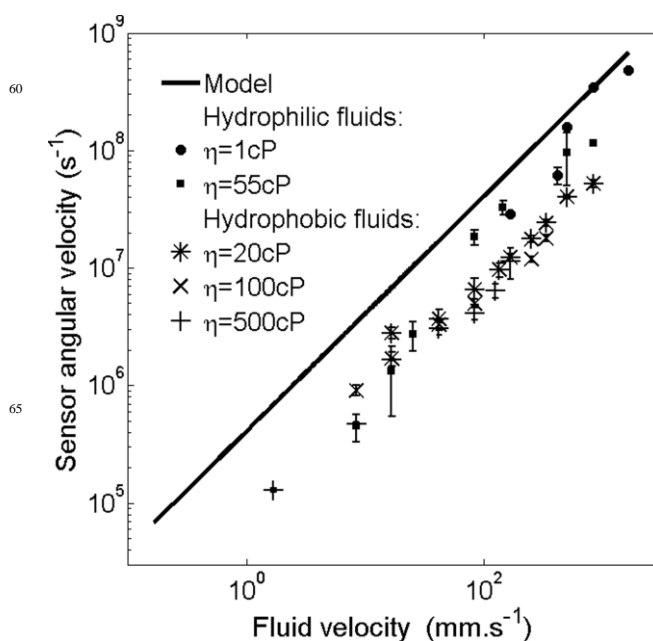


Fig. 2: Sensor angular velocity plotted versus the flow rate for five different fluids. Filled symbols: silicone oil (viscosities: 20, 100 and 500 cp). Open symbols, hydrophilic fluids: Water (viscosity 1cp) and PEG-DA prepolymer (viscosity 55 cp). All the plots collapse on a single master curve.

by solid friction between the sensor and the microchannel, and the maximum measurable flow rate by the weak resistance of the fluidic connection between the channel and the syringe pump. This important result demonstrates that the flow sensor rotation is independent of the fluid viscosity. We tested separately two types of fluids, hydrophilic ones, which are expected to swell the PEG based polymerized wheel, and hydrophobic ones, which are not expected to alter the mechanical properties of the sensor. As hydrophilic fluids, we used water + 0.1% Tween 20 surfactant (viscosity: 1cP) and the prepolymer solution itself (PEGDA 700 + 10% Darocur 1173) (viscosity: 55cP). As hydrophobic fluids, we used silicone oils. Fig. 2 shows that, at small fluid velocity, the linear relation between the measured angular velocity and the fluid flow rate is unaffected by the change in the fluid hydrophilicity over two decades of flow rate.

At high velocities, however, the data corresponding to hydrophilic fluids tend to deviate from the linear behaviour. Such non linear variations are typical of a fluid structure coupling. As confirmed by the observation of the helix shape, the viscous flow slightly deforms the sensor at high flow rate when hydrophilic liquids are used. It is likely that the swelling of the polymerized structure is responsible for this softening, which is not observed with silicone oils and other organic fluids. To circumvent this apparent limitation, two sensors made of two different monomers can be embedded in the sensor channel. Using only two different materials (one hydrophilic such as the PEG-DA and one hydrophobic one such as TMPTA) would provide a solution to extend the range of measurable flow rate from two to three decades independently of all the physico-chemical properties of the fluids.

Simulation and modeling

The simulation of the flow around a freely moving structure is a challenging task. However, the inspection of Fig. 1 reveals that the tangential velocity of the spinning sensor is much smaller than the fluid velocity. Therefore, at first order the flow field can be approximated by that around a non-mobile sensor having the same shape. The helix-shaped sensor shows the same behaviour the circle shaped-sensor (see Supplementary Material), so simulation was performed on a circle. This flow profile was computed using the finite element methods with COMSOL software. Fig. 3 shows the x -component of the fluid velocity averaged over the z -direction. The asymmetry in the flow profile along the y -direction is clearly visible and this asymmetry increases with the off-centering of the sensor axis (data not shown). As a result, the shear stress acting on the wheel can yield a non-zero driving torque on the cylindrical sensor. Another important observation is that the fluid velocity in the region comprised between the top (resp. bottom) of the sensor and the top (resp. bottom) of the channel is very small when the gap h is smaller than $(W-R)$. Moreover the corresponding velocity field is symmetric with respect to the (x,z) plane and thus does not contribute to the driving torque.

Going back to the case of a mobile sensor, the rotation of the sensor induces an additional Couette flow located within the horizontal lubrication layers above and below the sensor. The shearing of the fluid in this region results in a net torque, which resists to rotation, explaining why the tangential velocity of the wheel's edge is smaller than the fluid velocity. Since we are in a linear hydrodynamic regime, the global flow profile can be calculated by superimposing the flow calculated with a fixed velocity at the inlet and outlet of the channel, and a fixed wheel, and the flow obtained from a rotating sensor with zero velocity at the entrance and exit of the channel. Thus, the resistive torque can be calculated as in a Couette rheometer with a plane-plane geometry.

Modeling

Following the conclusions of the flow simulations above, we propose the following simplified model to analytically calculate the rotation of the sensor. As no external torque is applied on the sensor, the net viscous torque acting on the wheel must be zero (we implicitly ignore all inertial effect given the small size of the sensor). Thus, the angular velocity of the wheel is set by the balance of the driving torque, τ_D , acting on the wheel's vertical peripheral walls, and the resistive torque, τ_R , arising from the Couette flow in the lubricating layer. The tangential viscous force acting on the wheel scales as $\sim \eta R v_{\max}$, where v_{\max} is the fluid velocity in the red region in fig. 3. Assuming that all the fluid flows only on the left hand side of the wheel, volume conservation implies: $v_{\max} = QH^1/(W-2R)$. The driving torque is then approximated by:

$$\tau_D \sim \eta \frac{R^2}{H(W-2R)} Q$$

The torque balance condition thus leads to the response function of the flow sensor:

$$\omega = \frac{Q}{\pi(W-2R)R^2} \frac{h}{H}$$

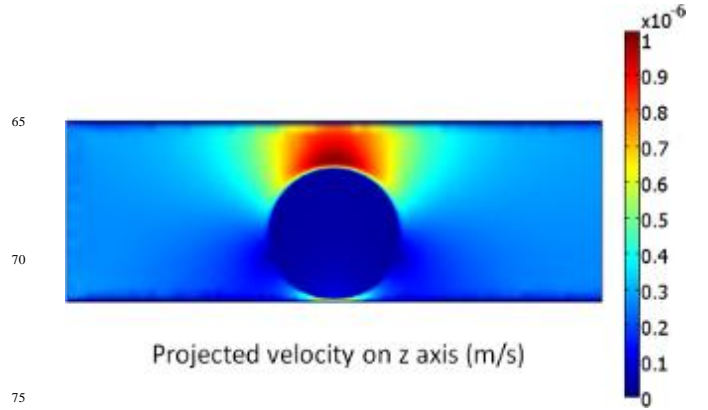


Fig. 3: z -projection of the x -component of the velocity field around a cylindrical wheel, for $H=20 \mu\text{m}$, $W=500 \mu\text{m}$, $h=5 \mu\text{m}$, $R=180 \mu\text{m}$ and $Q=100 \mu\text{l/min}$.

This estimate of the rotational velocity is in excellent agreement with the experimental data in Fig. 2. This simplified analysis thus provides a simple guideline for the sensor design. For instance, the above formula implies that scaling down the sensor would improve its sensitivity as the slope of the $Q(\omega)$ constitutive relation would be increased. In addition, to induce a strong driving torque, the distance between the wheel and the left channel wall: $\sim W-2R$ has to be as small as possible and kept much larger than the small distance between the wheel and the right wall to maximize the (asymmetric) fluid velocity past the sensor.

Discussion and conclusions

We have proposed a new paradigm for flow sensing in microfluidic channels, based on a rotating wheel asymmetrically positioned in a channel that provides a linear response to the flow rate, which is independent of the fluid viscosity. Wheels of different shapes were tested, and as expected in this high lubrication limit, the rotation velocity was independent of the detailed shape of the wheel, provided its thickness and outer diameter were kept constant (data not shown).

Using flow simulation and a simplified analytic model, we could predict quantitatively the linear response of the flow sensor. For fluids that do not swell the plastic sensor, the predicted values correctly fit the data without any adjustable parameter over the whole range of operation. For partially swelling fluids, rotation velocity of the sensor does not respond linearly to the flow in the high flow rate regime. This deviation is likely to be induced by a softening of the wheel, which induces a deformation. The use of a combination of wheels having different geometries and made of different polymers could thus provide a simple solution to extend the range of operation of the device.

In summary, this study demonstrates the possibility to use simple rotating wheels as universal flow sensors in microfluidics. This principle for flow sensing is well known in the macroscopic world, but it is new in the microfluidic world, and it can bring definite advantages as compared to other ones such as particle-based velocimetry or hot wire, notably its universal character.

Clearly, the technology will still require progress to maturity, before being employed as an industrial product. Our current data are still too noisy for high accuracy applications. We associate these errors at least in part to imperfections in the shape of the microchannels and wheel. Notably, optical defects in the microscope lithography process can yield geometrical defects in

the wheel itself. Indeed, we have noticed that the wheel rotation is not perfectly smooth. PDMS itself is a soft material, and the thickness of the microchannel can vary slightly from one experiment to the other, due to differences in the pressure used when sealing the channel (which induces into the PDMS a strain that is kept irreversible by the irreversible bonding of the two sides of the chip). Also, we could expect that a deformation of the microchannel by the hydrostatic pressure in the fluid could induce a modification of the fluid to wheel coupling. We checked by positioning the wheel at different places, that this was not the case in the range of flows used here, but in more general situations, the low elastic module of PDMS would certainly limit the range of linear response to moderate pressures. More generally, the photopolymerization and soft lithography processes used here is particularly convenient for laboratory use and fast prototyping, but industrial applications may require more conventional “MEMS” microfabrication methods, and harder materials, e.g. silicon, to yield smoother, more accurate systems usable in a larger range of operational conditions. We believe that the design strategy proposed here, and notably the validation of a simple analytical model with a good predictive value, will convey a useful guide in the design of such second generation systems. In the meantime, given their simplicity, soft lithography methods as demonstrated here already provide a simple and convenient solution for academic research and fast prototyping.

Experimental

Materials and microsystem

All photopolymerized structures shown in this work were prepared using 10% (w/w) solutions of Darocur 1173 (Sigma-Aldrich) initiator in (w/w) poly(ethylene glycol)(700) diacrylate (PEGDA, Sigma-Aldrich). All the sensors have a diameter of 360 μm. The UV illumination time is 0.35 second and the concentration ratios of monomer over photoinitiator is 10%. The PDMS devices were fabricated by pouring polydimethylsiloxane (PDMS, Sylgard 184, Dow Corning) on a silicon wafer containing positive-relief channels patterned in SU-8 photoresist (Microchem). The devices were rectangular channels of 500 μm width and 20 μm height, with 40 μm diameter posts every 4 mm. These devices were sealed with a glass slide spin-coated with PDMS to ensure that the prepolymer was only contacted with PDMS surfaces. The formation and the rotations of the sensors were visualized using a CCD camera (KP-M1EK-S10, Hitachi). Images were captured and processed using NIH Image software. The sensor height was measured with an AMBIOS XP1 profilometer.

Photopolymerization setup

Photomasks were designed in AUTOCAD 2006 and printed using a 24000 dpi high-resolution printer at Selba S.A. (Versoix, Switzerland). The mask was then inserted into the field-stop of the microscope (Zeiss Axiovert 200, tube lens magnification 4X). A 100 W HBO mercury lamp served as the source of UV light. Objective magnification was a 10_x (Zeiss Achromplan, 10X/0.25). A filter set allowing wide UV excitation (Excitation 365HT25, emission 400EFLP, Omega Optical) was used to select the desired wavelength. A VS25 shutter system (Uniblitz) driven by a computer-controlled D122 shutter driver provided pulses of UV light with the specified duration. Solutions were driven through the microfluidic device with a Kd Scientific 210P syringe pump.

Bibliography

- [1] D. Dendukuri, S. S. Gu, D. C. Pregibon, T. A. Hatton and P. S. Doyle, *Lab Chip*, 2007, 7, 818
 - [2] Ashauer, M., Glosch, H., Hedrich, F., Hey, N., Sandmaier, H., and Lang, W., *Sensors and Actuators A : Physical*, 1999, 73, 7-13.
 - [3] J. G. Santiago, S. T. Wereley, C. D. Meinhart, D. J. Beebe and R. J. Adrian, *Experiments in Fluids*, 1998, 25, 316–319.
 - [4] Attia, R., Pregibon D. C., Doyle, P.S. , Viovy , J.-L. , Bartolo, D., *Soft microflow sensors*, *Lab Chip*, 2009, 9, 1213- 1218
- ^a Laboratoire Physicochimie Curie, CNRS/UMR 168, 11 rue Pierre et Marie Curie, Paris, France. E-mail: ra2500@columbia.edu; jean-louis.viovy@curie.fr; Fax: (+33) 1 40 51 06 36; Tel: (+33) 1 56 24 68 44
- ^b Department of Chemical Engineering, Massachusetts Institute of Technology, 77 Massachusetts Ave., Cambridge, MA, 02139, USA. E-mail: pregibon@mit.edu; pdoyle@mit.edu
- ^c PMMH laboratory ESPCI-CNRS UMR 7636-Université Paris 6- Université Paris 7, 10, rue Vauquelin, 75231 Paris cedex 05, France. E-mail: denis.bartolo@espci.fr
- [†]Electronic supplementary information (ESI) available: Comparison between a helix-shaped sensor and a circular shaped sensor, in prepolymer ($\mu=55\text{cP}$). The angular velocity does not show any significant shift.